

# Diode-pumped Yb:KYW femtosecond laser frequency comb with stabilized carrier-envelope offset frequency

S.A. Meyer<sup>1,2</sup>, J.A. Squier<sup>3</sup>, and S.A. Diddams<sup>2,a</sup>

<sup>1</sup> Department of Physics, University of Colorado, 2000 Colorado Ave., Boulder, CO 80309, USA

<sup>2</sup> National Institute of Standards and Technology, 325 Broadway MS 847, Boulder, CO 80305, USA

<sup>3</sup> The Center for Microintegrated Optics for Advanced Bioimaging and Control, Colorado School of Mines, 1532 Illinois St., Golden, CO 80401, USA

Received 13 September 2007 / Received in final form 20 November 2007

Published online 23 January 2008 – © EDP Sciences, Società Italiana di Fisica, Springer-Verlag 2008

**Abstract.** We describe the detection and stabilization of the carrier envelope offset (CEO) frequency of a diode-pumped Yb:KYW (ytterbium-doped potassium yttrium tungstate) femtosecond oscillator that is spectrally centered at 1033 nm. The system consists of a diode-pumped, passively mode-locked femtosecond laser that produces 290 fs pulses at a repetition rate of 160 MHz. These pulses are first amplified, spectrally broadened and temporally compressed to 80 fs, and then launched into microstructured fiber to produce an octave-spanning spectrum. An  $f - 2f$  nonlinear interferometer is employed with the broadened spectrum to detect and stabilize the CEO frequency through feedback to the pump laser current. These results demonstrate that such a Yb-doped tungstate laser can provide an efficient, compact, high-repetition-rate optical frequency comb with coverage from 650–1450 nm.

**PACS.** 42.65.Re Ultrafast processes; optical pulse generation and pulse compression – 42.55.Xi Diode-pumped lasers

## 1 Introduction

There is little doubt of the significant impact that femtosecond laser optical frequency combs have already made in the areas of precision optical metrology, optical clocks, and precision spectroscopy [1, 2]. However, the pursuit of the best laboratory implementation is a continuous one, and will likely be application dependent. Interestingly, among the hundreds of femtosecond lasers that have been described in the literature, only a handful have been self-referenced and applied to optical frequency metrology experiments. From a broader perspective, this apparent under-sampling of the available resources would suggest there is likely something to be gained by exploring new femtosecond laser systems for use in frequency metrology- and spectroscopy-related experiments. From a more focused perspective, there are certain advantages and drawbacks to existing frequency comb systems that one would like to optimize for each particular application (e.g. size, cost, low repetition rate, excess noise, transportability, etc.).

In this article, we describe a promising frequency comb system based on an ytterbium-doped potassium yttrium tungstate femtosecond laser ( $\text{Yb:KY(WO}_4\text{)}_2$  or more com-

monly Yb:KYW). The frequency comb consists of a direct-diode-pumped femtosecond oscillator, a low-power fiber amplifier, continuum generation in microstructured fiber, and subsequent  $f - 2f$  self-referencing leading to control of the carrier-envelope offset frequency [3, 4]. As will be discussed in the following, this system has the particular advantage of being compact, low cost, robust, low power, and power efficient, which was part of our motivation for developing it. Our initial results show relatively low levels of frequency noise on the generated frequency comb, indicating that with reasonable improvements to the servo control the frequency noise properties of a Yb:KYW frequency comb should be reducible to levels already achieved with other systems.

Two of the most widely used femtosecond laser frequency combs are based on Ti:sapphire and Er-doped fiber laser oscillators. For frequency metrology, Ti:sapphire frequency combs have the principle advantages of high repetition rates (up to 6 GHz [5]), very low residual frequency noise [6–9], and octave-spanning spectra directly from the laser [10–12]. The main disadvantages of the Ti:sapphire frequency comb are its bulk-optic design, requiring careful alignment and clean operating conditions, and the relatively large, expensive, and inefficient pump source at 532 nm. These are not fundamental limitations, but rather practical design constraints that may (or may

<sup>a</sup> e-mail: sdiddams@boulder.nist.gov

not) be an issue in various applications. For example, a Ti:sapphire based comb can also operate with a low-power (1 W), small-footprint pump source [13]. Frequency combs based on Er-doped fiber lasers offer an attractive alternative to Ti:sapphire [14–17]. Such femtosecond fiber lasers are pumped directly with diodes at 980 nm or 1490 nm, making them efficient and compact. Emission at 1550 nm makes them well suited for fiber optic transmission, and the use of integrated fiber components minimizes alignment issues while taking advantage of the wide variety of robust and low-cost components designed for telecommunications systems. Moreover, improved active stabilization techniques have reduced the close-to-carrier frequency noise to similar levels achieved with Ti:sapphire lasers [18, 19]. However, the main drawbacks of fiber frequency combs are the need for external amplification, relatively low repetition rate (which has thus far been limited to a few hundred megahertz [20]), and the reduced spectral overlap with several promising optical frequency standards. For some applications, the predicted higher noise-floor [21], associated with the lower cavity quality factor ( $Q$ ) and amplified spontaneous emission in the laser and external fiber amplifier, could also be detrimental.

While there has been extensive development of femtosecond lasers based on Yb-doped crystals, fibers and glasses, to our knowledge the application and properties of these systems as frequency comb sources has been investigated in only a few cases [22, 23]. Here we focus our attention on Yb:KYW, but one could expect that similar arguments would apply to many of the other Yb-doped hosts. As a femtosecond laser source, Yb-doped hosts have much to offer [24]. Importantly, they can be directly pumped by common high-brightness laser diodes. The quantum defect is low, which leads to higher efficiencies and lower thermal loads on the crystal. The low lying states of the Yb ion have a relatively simple energy structure that avoids problems such as concentration quenching and excited state absorption, thus permitting high doping concentrations in glasses and crystalline hosts. Passive mode-locking via Kerr Lens Modelocking (KLM) [25, 26] and/or a semiconductor saturable absorber mirror (SESAM) [27–29] is now routine in such Yb lasers, making for robust operation. Though high power versions have been demonstrated [30], our goals of compactness, efficiency and high repetition rate led us to develop a system pumped with single-mode fiber coupled, low-power (<1 W) laser diodes. Repetition rates up to 300 MHz have been achieved with Yb:KYW using KLM [25], and still higher repetition rates should be achievable. The emission bandwidth of crystals such as Yb:KYW is significantly narrower than that of Ti:Sapphire, so that the oscillating bandwidth typically supports minimum pulse durations of around 100 fs (a value comparable to those of Er:fiber sources). However, spectral broadening from below 600 nm to 1500 nm can be efficiently accomplished in nonlinear optical fibers, such as microstructured and tapered fibers [22, 31, 32]. As a result, an Yb frequency comb has good spectral overlap with many of the wavelengths important for optical frequency standards presently under development. These

include Hg+ (1126 nm), Al+ (1070 nm), Yb (1158 nm), Sr (699 nm), Sr+ (674 nm), Ca (657 nm), Yb+ (872 nm, 934 nm), In+ (947 nm), H (973 nm). Finally, when compared to Yb-fiber lasers, the laser presented here has lower cavity losses and a correspondingly higher cavity  $Q$ , which should result in lower phase noise on the frequency comb. This could be a factor for some experiments, such as low-noise microwave generation [9] and harmonic frequency comb generation below 100 nm by use of an external enhancement cavity [23]. In addition, the high efficiency and low power requirements may be well-suited for transportable field applications. Together, these factors make Yb:KYW an interesting frequency comb system to study as well as a promising alternative to existing frequency comb systems for many applications.

## 2 Experimental details

### 2.1 Yb:KYW oscillator

Our design is based on a diode-pumped Yb:KYW solid-state femtosecond laser. The Yb:KYW crystal has a strong but sharp absorption peak at 981 nm ( $\Delta\lambda = 4$  nm), a wavelength where high power laser diodes are readily available. It emits in the spectral range 1020–1060 nm and has been shown to exhibit pulses as short as 71 fs [26]. Our laser cavity design is shown in Figure 1. A 10-at.%, 1 mm long Yb:KYW crystal is Brewster cut for the pump and laser fields being polarized parallel to the “a” crystal axis ( $E \parallel a$ ). The crystal is pumped by two PM-fiber coupled, fiber Bragg grating stabilized, 600 mW laser diodes. The crystal is mounted on a copper mount with indium foil used to make good thermal contact. The crystal is not actively cooled, although cooling could lead to higher inversions in the gain medium, as the lower lasing levels are the higher Stark levels of the ground state, which can be populated at finite temperature. The femtosecond oscillator uses a modified  $x$ -fold cavity with two  $R = 5$  cm focussing mirrors. In one arm an  $R = 20$  cm mirror focusses the light onto a semiconductor saturable absorbing mirror (SESAM) end mirror to initiate and stabilize mode-locking [33]. Two SF10 Brewster prisms in the second arm are used for dispersion compensation with the 5% output coupler as the end mirror in this arm. A  $-250$  fs $^2$  Gire-Tournois Interferometer (GTI) mirror provides extra negative dispersion and is used as a folding mirror in this same arm. One advantage of the SESAM mode-locked system is that it is self-starting. Moreover, even without significant attention given to engineering details, the laser operates reliably over extended periods (weeks) without the need for alignment.

With the 1.2% modulation depth SESAM in the cavity, mode-locking is self-starting and leads to pulses with an intensity autocorrelation as shown in Figure 2. This implies 290 fs pulses which are at a repetition rate of 160 MHz with 240 mW average output power. This pulse length is long compared with previous values as low as 107 fs for  $E \parallel a$  operation [25], however, in this present configuration we were unable to shorten the pulse further.

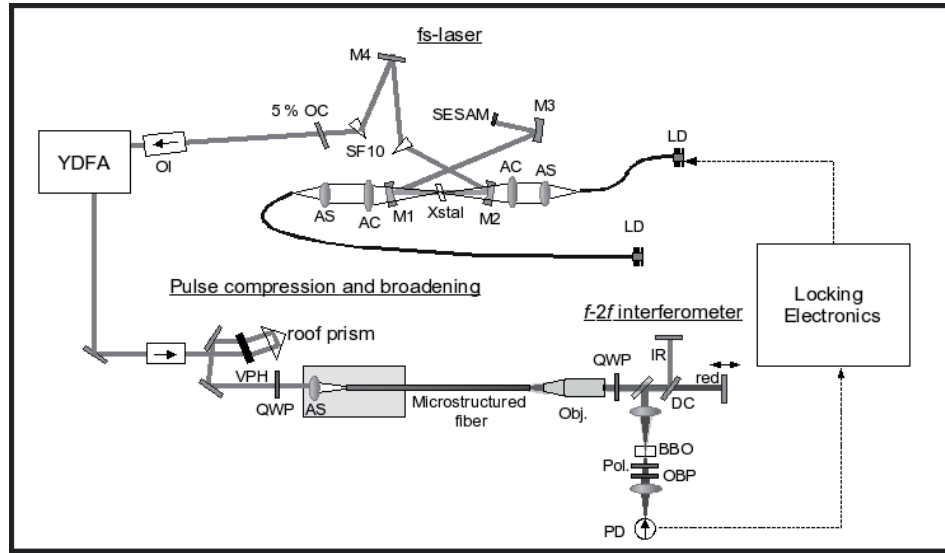


**Fig. 1.** A schematic diagram of the set-up is shown. The 1 mm thick, 10-at.% Yb:KYW crystal (Xstal) is pumped by two PM coupled, fiber bragg grating stabilized laser diodes (LD). The cavity is  $x$ -folded, with SF10 prisms for dispersion compensation. M1 and M2 have  $R = 5$  cm, M3 has  $R = 20$  cm and M4 is a GTI mirror with  $-250$  fs $^2$  of dispersion. A 1.2% modulation depth SESAM and 5% output coupler (OC) are used. The fs-laser output goes through an optical isolator (OI) and is amplified in a Yb-doped fiber amplifier (YDFA) and compressed by a volume phase hologram (VPH) and roof prism. The output is spectrally broadened in a microstructured fiber and is sent to the  $f - 2f$  interferometer for CEO detection. The infra-red (IR) and red light are separated and recombined with a dichroic mirror (DC). The IR is then doubled in a BBO crystal and the  $f_0$  beat is detected on a photodiode (PD) and locked using a phase locked loop. AC = achromatic lens, AS = aspheric lens, YDFA = Yb-doped fiber amplifier, QWP = quarter wave-plate, Pol. = polarizer, OBP = optical band-pass filter, Obj. = microscope objective.

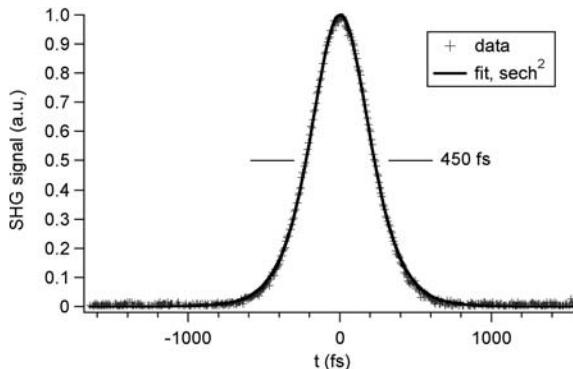


**Fig. 2.** A sample intensity autocorrelation trace and sech $^2$  fit of the output of the Yb:KYW oscillator is shown. The FWHM implies a pulse length of 290 fs.

Attempts to further shorten the pulse by pushing the net cavity dispersion closer to zero (inserting more prism glass) leads to the onset of multiple pulsing. Along these lines, the shortest pulse of 290 fs also required increasing the output coupler from 2.4% to the present 5%, and focusing less tightly onto the SESAM with the  $R = 20$  cm in place of an initial  $R = 10$  cm. Although shorter pulse lengths should in principle be possible from this crystal, the pulse lengths we obtained still allowed us to proceed with CEO detection and locking, as described below.

We note that to obtain the 290 fs pulse length the laser was operated with what amounts to a significantly large net negative dispersion of around  $-1200$  fs $^2$  (for one

round trip in the cavity). The largest contribution arose from the prisms and GTI mirror which provided approximately  $-2000$  fs $^2$ . Positive dispersion from the laser crystal amounted to only  $+200$  fs $^2$  for each pass through the 1 mm crystal at 1030 nm. This was measured by the white light interferometer technique described in [34]. The SESAM,  $R = 20$  cm mirror and output coupler have dispersion values close to zero. We also measured the dispersion of the  $R = 5$  cm pump mirrors to be approximately  $+100$  fs $^2$  per bounce, although this value oscillated strongly in the 1020–1030 nm region. This is most likely due to the proximity of the 980 nm pump laser transmission window in the high reflective coating, which without careful mirror design can cause erratic dispersion behavior near this sharp edge. For the repetition rate of 160 MHz demonstrated here, prisms and subsequently long cavities can readily provide large negative dispersion, but for higher repetition rates the cavity dispersion and its influence on the pulse width will need to be better understood and addressed.

## 2.2 Amplification, compression, and spectral broadening

The output of this Yb:KYW oscillator is amplified with a single-mode Yb-doped fiber amplifier. The pulses are not intentionally chirped before the amplifier so that, in addition to the amplification, some spectral broadening is seen. With 120 mW coupled into the amplifier, an output power of 360 mW is measured, and subsequently compressed

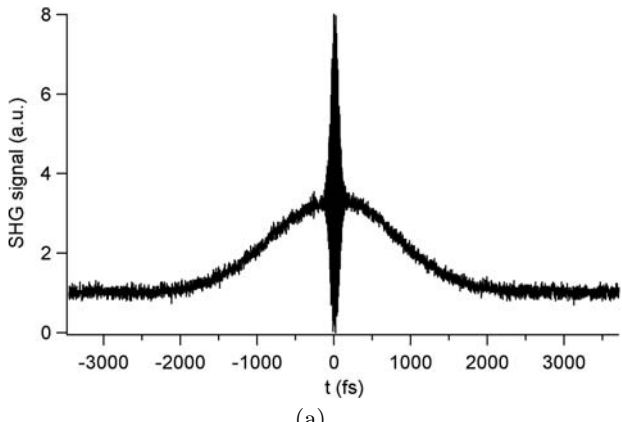


**Fig. 3.** Interferometric autocorrelation trace of the chirped pulse after amplification is shown in (a). The compressed pulse, shown in (b), has a FWHM of 80 fs. The broadening of the laser spectrum in the amplifier is shown for various amplifier output powers in (c).

with a volume phase hologram (VPH) grating and roof prism compressor (see Fig. 1) from 2 ps out of the amplifier to 80 fs, as shown in Figure 3. The extra bandwidth from the spectral broadening in the amplifier, as shown for various output powers from the amplifier in Figure 3c, allows pulses shorter than those from the Yb:KYW oscillator alone. The VPH grating is 99% efficient and the over-

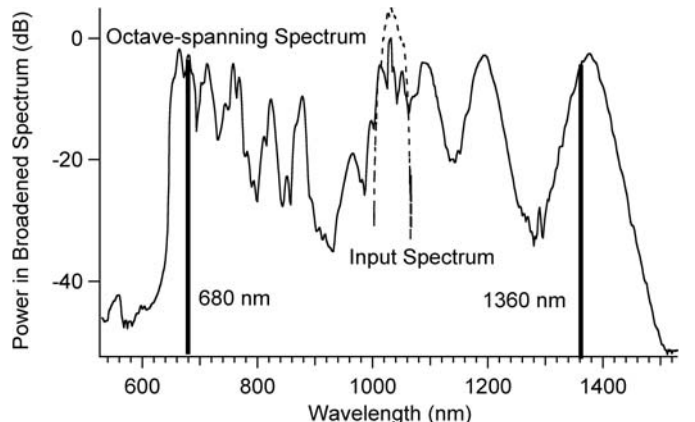


**Fig. 4.** The octave-spanning spectrum seen after broadening in a microstructured fiber is shown, along with the spectrum of the amplifier output for comparison. The peak around 680 nm has twice the frequency of the peak at 1360 nm, so that these two peaks can be used for  $f - 2f$  CEO detection.

all compressor efficiency is 85%. The beam passes through the compressor only once, so the output beam is spatially chirped. However, this chirp is small enough to not visibly distort the output beam shape and does not apparently degrade the focusing into the microstructured fiber.

A one meter long microstructured nonlinear fiber with a zero dispersion wavelength of 945 nm and a core diameter of  $3.2 \mu\text{m}$  is used to broaden the output from the pulse compressor to the octave-spanning spectrum shown in Figure 4, which has strong peaks at  $\sim 680$  nm and  $\sim 1360$  nm for  $f - 2f$  detection. We tried several different fibers and found that this fiber gave the best broad spectrum at the powers and pulse lengths available. An aspheric lens was used to successfully couple 115 mW of light into the fiber and an achromatic microscope objective was used to collimate the output from the fiber, as chromatic aberrations from an aspheric lens would be detrimental to mode-matching the broadened light at both ends of the spectrum. We note that we were also able to obtain an octave-spanning spectrum using the same fiber with the direct oscillator output when the cavity length was extended to allow a 91 MHz repetition rate, which gave substantially shorter output pulse lengths of 160 fs and an average coupled power of 73 mW [36]. However our inclination toward higher repetition rates prompted us to use a shorter cavity and thus the alternative route presented here.

### 2.3 $f - 2f$ CEO detection and stabilization

In order to stabilize the spectrum from a mode-locked laser both the repetition rate,  $f_{rep}$ , and the offset frequency,  $f_0$ , must be stabilized. To measure  $f_{rep}$  one must simply put a photodiode in the beam path;  $f_{rep}$  can then be stabilized by controlling the length of the cavity with a piezoelectric transducer behind one of the mirrors. To stabilize  $f_0$  one must first measure it, and the most common way to do this

is with an  $f - 2f$  interferometer. The offset frequency,  $f_0$ , is simply the common offset of the evenly spaced comb of optical frequencies from harmonics of  $f_{rep}$ . Thus for any mode,  $n$  of a mode-locked laser with repetition rate  $f_{rep}$ , the following is true:

$$f_n = f_0 + n f_{rep}.$$

If the  $n$ th comb line is doubled and interfered with the  $2n$ th comb line on a detector the beat signal will be at  $f_0$ . This is an RF frequency that can be phase locked to a stable reference frequency with the laser pump power as an actuator.

The collimated octave spectrum is sent into the  $f - 2f$  interferometer shown in Figure 1 for detection of the  $f_0$  beatnote. The IR light is separated from the red light by a dichroic mirror. A translation stage in one arm is used to match the IR and red pulses in time at the detector, as they become separated due to dispersion in the various optics. The interferometer end mirrors are tipped slightly down so that the light heading back through the beam-splitter can be picked off and sent to the BBO crystal used to double the IR light with type I phase matching. A subsequent polarizer projects the doubled light and the undoubled red light onto a common polarization axis. The  $f_0$  beatnote is then detected on a photodiode, after an optical bandpass filter removes excess light. The spectrum of the photodiode signal was measured with an RF spectrum analyzer and is shown in Figure 5. The  $f_0$  signal has a signal to noise ratio (SNR) of 34 dB in a 100 kHz resolution bandwidth. The noise floor on the  $f_0$  beat signal in Figure 5a is above the shot noise limit and the electronics noise floor and shows evidence of excess noise from supercontinuum generation [35, 37]. We note the relatively clean spectrum of the unlocked  $f_0$  spectrum without the Lorentzian-like wings commonly observed in fiber laser systems [16, 21, 22].

A PLL locks  $f_0$  to a stable RF reference by controlling the current to one of the laser diodes. In this system the CEO frequency can be continuously tuned with very small changes to the prism insertion, which allows us to move the offset to a convenient frequency for the electronics. The  $f_0$  signal at 266 MHz is first filtered with a tunable bandpass filter, then amplified. The frequency of the signal is then divided by 64. The phase difference between a stable reference and  $f_0/64$  is produced with a digital phase detector. This error signal is filtered and amplified with a loop filter and sent to the current modulation port of one of the pump laser diode current controllers. The resulting  $f_0$  carrier signal with the loop closed and locked is shown in Figure 5c. As expected, when phase-locked the linewidth is limited by the RF spectrum analyzer used for the measurement. More complete information on the performance of the phase-lock is obtained from a vector signal analyzer that measures the power spectral density (PSD) of residual phase fluctuations on the locked offset frequency, as shown in Figure 6. An integrated phase noise of 1.7 radians (5 Hz to 4 MHz) is calculated from the PSD. When the system is locked and the  $f_0$  beat is sent to a frequency counter, the standard deviation of the frequency

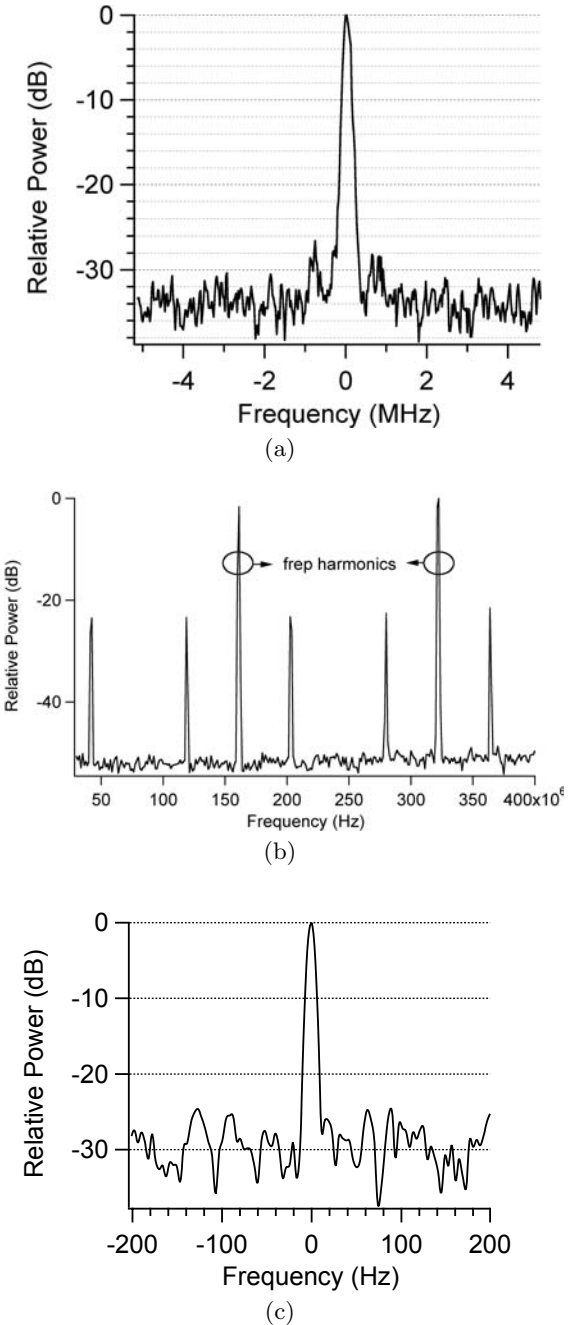


**Fig. 5.** The RF spectrum of the unlocked signal on the PD, both zoomed in, (a), and zoomed out, (b) and the locked (c)  $f_0$  beatnote are shown. The unlocked beat signal has a SNR of 34 dB in a 100 kHz resolution bandwidth. The locked carrier signal is shown at 10 Hz resolution bandwidth and has an instrument limited FWHM.

fluctuations is  $\sigma_{f_0} = 2$  mHz (limited by the counter) for 1 s averaging and 137 points total. Over a 10 minute period there were several transient slips in the phase-lock due to unknown sources, but the millihertz level standard deviation when stably locked indicates that this system is quite capable of producing a highly stable optical frequency comb, once the repetition rate is also stabilized.

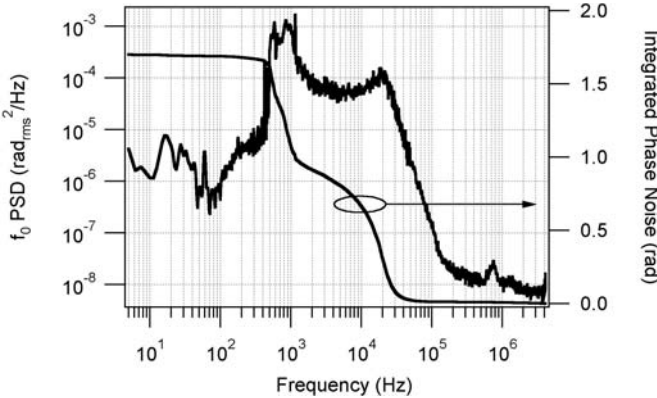


**Fig. 6.** The power spectral density (PSD) of residual phase noise fluctuations on the locked  $f_0$  signal is shown, along with the integrated phase noise, which is 1.7 radians over the interval shown.

While the performance of the  $f_0$  phase lock is already sufficient for frequency counting experiments, the integrated phase noise is still about a factor of 10 greater than what is typically achieved in Ti:sapphire and Er-fiber systems, indicating further improvements to this lock are necessary. Moreover, because the noise on the pump lasers has been shown to be a significant source of noise in the CEO frequency of most frequency comb systems [38,39], we measured the frequency-dependent transfer functions of modulation of the pump laser diode current to the laser diode output power, the Yb:KYW oscillator output power, and  $f_0$ . For the laser diode and Yb:KYW output powers this is accomplished by inserting a photodiode at the respective output and using a network analyzer to record the amplitude fluctuations as the diode current is modulated by the analyzer's noise source. However, measuring the frequency response of  $f_0$  to diode current modulation requires the use of a frequency-to-voltage conversion. In this case, a delay line frequency discriminator was used to obtain an output voltage that is proportional to the frequency fluctuations. As seen in Figure 7a, all three elements tested have a roll-off of about 20–30 kHz in their response. The frequency response of the pump laser diode power has a roll-off near 30 kHz, which is consistent with the specifications of the laser diode driver's response to input modulation, but should not represent a fundamental limit. The response of the Yb:KYW power and  $f_0$  are essentially identical, and have modulation bandwidths only slightly lower than that of the pump laser itself. Presumably, the response of  $f_0$  is closely tied to gain and laser power dynamics in the Yb:KYW laser. One also notes the correspondence between the 20 kHz roll-off of the response of  $f_0$  to pump current modulation and the sharp drop in the PSD of Figure 6. Correlation between the large peak at 1 kHz in the  $f_0$  PSD and amplitude noise on the pump diodes has not yet been investigated. Together, these data suggest that further reduction of the free running laser noise around 1 kHz and slightly larger servo bandwidth are likely the key to decreasing the phase noise in the  $f_0$

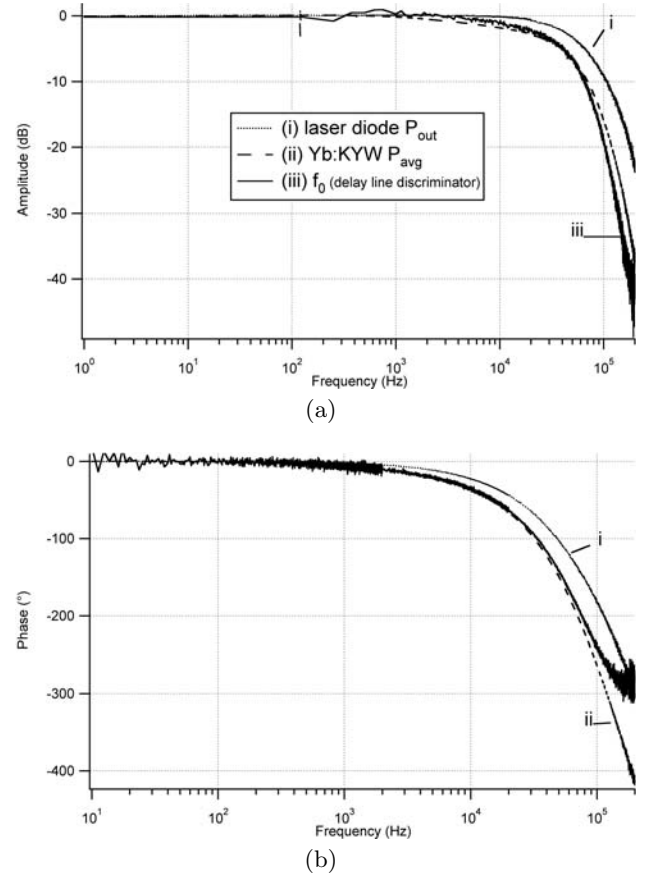


**Fig. 7.** The frequency-dependent response of the pump laser power, Yb:KYW power, and  $f_0$  to modulation of the 981 nm diode current as measured using a network analyzer. The amplitude response is shown on the top and the phase response is shown on the bottom. The response of the laser diode (i), the Yb:KYW fs-oscillator average power (ii) and  $f_0$  beat signal (iii) are shown. The three amplitude curves are normalized to the same maximum value at 0 Hz. The response of  $f_0$  was measured using a delay-line discriminator.

lock. Towards this end, it will be useful to employ an appropriate phase lead inside the servo loop, as successfully demonstrated for Er-fiber lasers [39].

### 3 Discussion and conclusions

In this article we report a diode-pumped, CEO frequency stabilized Yb:KYW femtosecond laser frequency comb. The femtosecond laser was built, the output was amplified, re-compressed, broadened to an octave-spanning spectrum in a microstructured fiber, and the CEO frequency was detected and stabilized with an  $f - 2f$  interferometer and feedback to the pump laser current. The phase-locked CEO frequency, although not as stable as the well-developed Ti:sapphire and Er-fiber frequency combs, has phase noise well below  $\pi$  radians. Improvements to this system would include identification of the source of glitches on the offset frequency as well as increasing the

bandwidth of the  $f_0$  servo, as discussed above. Optimization of the length of the nonlinear microstructured fiber could lead to improved signal to noise ratio on  $f_0$ . One must also detect and lock the repetition rate of the laser to have a fully stabilized comb. It should be straightforward to control  $f_{rep}$  with a microwave reference, but lower noise levels will be attained by stabilization to an optical reference. Finally, it will be interesting to attempt to increase the repetition rate of the laser towards the gigahertz range, while keeping the pulse length as close to 100 fs as possible. Though SESAM mode-locked solid-state lasers (Nd:YVO<sub>4</sub>) of repetition rates up to 160 GHz have been demonstrated [40], these systems have much lower peak powers, mostly due to the long pulse length of  $\sim 10$  ps, which would make continuum generation difficult. However, as mentioned previously, KLM mode-locking of Yb:KYW has been demonstrated at about a 300 MHz repetition rate with  $\sim 100$  fs pulses, and given the relatively large nonlinear refractive index for Yb:KYW of  $8.7 \times 10^{-16} \text{ cm}^2/\text{W}$  [41] (compared to  $3 \times 10^{-16} \text{ cm}^2/\text{W}$  for Ti:sapphire [42]), sufficient nonlinear phase modulation required for higher repetition rate KLM femtosecond operation should be possible with the present 1.2 W of pump power.

This paper is a contribution of an agency of the US government and not subject to copyright in the US. Financial support was provided by the Defense Advanced Research Projects Agency (DARPA) and the National Institute of Standards and Technology (NIST). J. Squier further acknowledges the support of the National Institute of Biomedical Imaging and Bio-Engineering (NIBIB) under grant EB003832. The authors thank Nathan Newbury and Leo Hollberg for their contributions to this work as well as Sara Trowbridge and Michael Thiel for their efforts in the early development of the Yb:KYW oscillator. Finally, we appreciate the helpful comments on this manuscript provided by Thomas Schibli and Ingmar Hartl.

#### Note added in proof

We have recently eliminated the source of glitches in the offset frequency phase lock and have reduced the integrated phase noise in this lock to 0.3 rad.

## References

1. J.L. Hall, Rev. Mod. Phys. **78**, 1279 (2006)
2. T.W. Hänsch, Rev. Mod. Phys. **78**, 1297 (2006)
3. H.R. Telle, G. Steinmeyer, A.E. Dunlop, J. Stenger, D.H. Sutter, U. Keller, Appl. Phys. B **69**, 327 (1999)
4. D.J. Jones, S.A. Diddams, J.K. Ranka, A. Stentz, R.S. Windeler, J.L. Hall, S.T. Cundiff, Science **288**, 635 (2000)
5. A. Bartels, R. Gebs, M. Kirchner, S. Diddams, Opt. Lett. **32**, 2553 (2007)
6. J. Stenger, H. Schnatz, Ch. Tamm, H.R. Telle, Phys. Rev. Lett. **88**, 073601 (2002)
7. L.-S. Ma, Z. Bi, A. Bartels, L. Robertsson, M. Zucco, R.S. Windeler, G. Wilpers, C. Oates, L. Hollberg, S.A. Diddams, Science **303**, 1843 (2004)
8. A. Bartels, C.W. Oates, L. Hollberg, S. Diddams, Opt. Lett. **29**, 1081 (2004)
9. J.J. McFerran, E.N. Ivanov, A. Bartels, G. Wilpers, C.W. Oates, S.A. Diddams, L. Hollberg, Elect. Lett. **41**, 650 (2005)
10. U. Morgner, R. Ell, G. Metzler, T.R. Schibli, F.X. Krtner, J.G. Fujimoto, H.A. Haus, E.P. Ippen, Phys. Rev. Lett. **86**, 5462 (2001)
11. O. Mücke, R. Ell, A. Winter, J.-W. Kim, J. Birge, L. Matos, F. Kärtner, Opt. Express **13**, 5163 (2005)
12. T. Fortier, A. Bartels, S. Diddams, Opt. Lett. **31**, 1011 (2006)
13. M.S. Kirchner, T.M. Fortier, A. Bartels, S.A. Diddams, Opt. Express **14**, 9531 (2006)
14. F. Tauser, A. Leitenstorfer, W. Zinth, Opt. Express **11**, 594 (2003)
15. F.-L. Hong, K. Minoshima, A. Onae, H. Inaba, H. Takada, A. Hirai, H. Matsumoto, T. Sugiura, M. Yoshida, Opt. Lett. **28**, 1516 (2003)
16. B. Washburn, S. Diddams, N. Newbury, J.W. Nicholson, M.F. Yan, C.G. Jørgensen, G. Carsten, Opt. Lett. **29**, 250 (2004)
17. T.R. Schibli, K. Minoshima, F.-L. Hong, H. Inaba, A. Onae, H. Matsumoto, I. Hartl, M.E. Fermann, Opt. Lett. **29**, 2467 (2004)
18. W.C. Swann, J.J. McFerran, I. Coddington, N.R. Newbury, I. Hartl, M.E. Fermann, P.S. Westbrook, J.W. Nicholson, F.S. Feder, C. Langrock, M.M. Fejer, Opt. Lett. **31**, 3046 (2006)
19. I. Coddington, W.C. Swann, L. Lorini, J.C. Bergquist, K.S. Feder, Y. Le Coq, J.W. Nicholson, C.W. Oates, Q. Quraishi, P.S. Wesbrook, S.A. Diddams, N.R. Newbury, Nature Photonics **1**, 283 (2007)
20. T. Wilken, T.W. Hänsch, R. Holzwarth, P. Adel, M. Mei, presented at *CLEO/QELS 2007*, paper CMR3
21. N.R. Newbury, W.C. Swann, J. Opt. Soc. Am. B **24**, 1756 (2007)
22. I. Hartl, M.E. Fermann, P. Pal, W.H. Knox, in *Conference on Lasers and Electro-Optics/Quantum Electronics and Laser Science Conference and Photonic Applications Systems Technologies*, OSA Technical Digest Series (CD) (Optical Society of America, 2007), paper CMU2
23. I. Hartl, A. Marcinkevicius, M.E. Fermann, T.R. Schibli, D.D. Hudson, D.C. Yost, J. Ye, to appear in Opt. Lett.
24. C. Hönninger, R. Paschotta, M. Graf, F. Morier-Genoud, G. Zhang, M. Moser, S. Biswal, J. Nees, A. Braun, G.A. Mourou, I. Johannsen, A. Giesen, W. Seeber, U. Keller, Appl. Phys. B **69**, 3 (1999)
25. A. Lagatsky, C. Brown, W. Sibbett, Opt. Express **12**, 3928 (2004)
26. H. Liu, J. Nees, G. Mourou, Opt. Lett. **26**, 1723 (2001)
27. F. Brunner, G.J. Spuler, J. Aus der Au, L. Krainer, F. Morier-Genoud, R. Paschotta, N. Lichtenstein, S. Weiss, C. Harder, A.A. Lagatsky, A. Abdolvand, N.V. Kuleshov, U. Keller, Opt. Lett. **25**, 1119 (2000)
28. P. Klopp, V. Petrov, U. Griebner, G. Erbert, Opt. Express **10**, 108 (2002)
29. A.A. Lagatsky, E.U. Rafailov, C.G. Leburn, C.T.A. Brown, N. Xiang, O.G. Okhotnikov, W. Sibbett, Elect. Lett. **39**, 1108 (2003)

30. F. Brunner, T. Südmeyer, E. Innerhofer, F. Morier-Genoud, R. Paschotta, V.E. Kisel, V.G. Shcherbitsky, N.V. Kuleshov, J. Gao, K. Contag, A. Giesen, U. Keller, Opt. Lett. **27**, 1162 (2002)
31. Y. Deng, F. Lu, W. Knox, Opt. Express **13**, 4589 (2005)
32. J. Teipel, D. Türke, H. Giessen, A. Killi, U. Morgner, M. Lederer, D. Kopf, M. Kolesik, Opt. Express **13**, 1477 (2005)
33. U. Keller, K.J. Weingarten, F.X. Kärtner, D. Kopf, B. Braun, I.D. Jung, R. Fluck, C. Höninger, N. Matuschek, J. Aus der Au, IEEE J. Quant. Elect. **2**, 435 (1996)
34. S.A. Diddams, J.-C. Diels., J. Opt. Soc. Am. B **13**, 1120 (1996)
35. J.N. Ames, S. Ghosh, R.S. Windeler, A.L. Gaeta, S.T. Cundiff, Appl. Phys. B **77**, 279 (2003)
36. S.A. Meyer, J.A. Squier, S.A. Diddams, presented at *CLEO/Europe-IQEC*, poster JSIII-2-MON
37. K.L. Corwin, N.R. Newbury, J.M. Dudley, S. Coen, S.A. Diddams, B.R. Washburn, K. Weber, R.S. Windeler, Appl. Phys. B **77**, 267 (2003)
38. W.C. Swann, B.R. Washburn, N.R. Newbury, Opt. Express **13**, 10622 (2005)
39. J.J. McFerran, W.C. Swann, B.R. Washburn, N.R. Newbury, Appl. Phys. B **86**, 219 (2006)
40. L. Krainer, R. Paschotta, S. Lecomte, M. Moser, K.J. Weingarten, U. Keller, IEEE J. Quant. Elect. **38**, 1331 (2002)
41. K.V. Yumashev, N.N. Posnov, P.V. Prokoshin, V.L. Kalashnov, F. Mejid, I.G. Poloyko, V.P. Mikhailov, V.P. Kozich., Opt. Quantum Electron. **32**, 43 (2000)
42. R. Desalvo, A.A. Said, D.J. Hagan, E.W. Van Stryland, M. Sheik-Bahae, IEEE J. Quant. Elect. **32**, 1324 (1996)